The sensitivity of geomagnetic reversal frequency to core-mantle boundary heat flux magnitude and heterogeneity

Maurits Metman[1], *Lennart de Groot*[2], *Cedric Thieulot*[1,3], *Andrew Biggin*[4], *Wim Spakman*[1,3]

[1]Department of Earth Sciences, Utrecht University, Utrecht, The Netherlands, [2]Paleomagnetic laboratory Fort Hoofddijk, Utrecht University, Utrecht, the Netherlands, [3]CEED, University of Oslo, Norway, [4]Geomagnetism Laboratory, Oliver Lodge laboratories, University of Liverpool, Liverpool, UK

Universiteit Utrecht

This poster participates in OSP

Outstanding Student Poster Contest

Introduction

For a number of decades the core-mantle boundary (CMB) heat flux has been thought to be a key parameter controlling the geomagnetic field. A CMB heat flow increase is assumed to destabilize the geodynamo, increasing and decreasing the reversal frequency and dipole moment, respectively. The opposite case where a CMB flux decrease induces a relatively high dipole moment, as well as a low reversal frequency, would correspond to the characteristics of a superchron (Biggin et al., 2012).

Moreover, the temporal and spatial heat flux distribution across the CMB also appears to have an influence on the geomagnetic reversal frequency. For example, the amount of heat flux heterogeneity may also be associated with a destabilization of the dynamo, increasing the reversal frequency (Olson et al., 2010).

In this work we set out to assess:

1. what combination of magnitude and heterogeneity best reproduces the geomagnetic record on the 10 Myr timescale;

2. how the geomagnetic field intensity and reversals are predominantly sensitive to CMB heat flux magnitude or heterogeneity.

CMB heat flow models + parameter evolution
=
reversal record?

Methods

Using the PARODY-JA code, written by Emmanuel Dormy and Julien Aubert, we numerically solve the equations:

$$\frac{\partial \mathbf{u}}{\partial t} + \mathbf{u}\cdot\nabla\mathbf{u} + 2\mathbf{e}_z \times \mathbf{u} + \nabla P = Ra_Q \frac{\mathbf{r}}{r_o} C + (\nabla \times \mathbf{B}) \times \mathbf{B} + E\nabla^2 \mathbf{u}$$

$$\frac{\partial \mathbf{B}}{\partial t} = \nabla \times (\mathbf{u} \times \mathbf{B}) + \frac{E}{Pm}\nabla^2 \mathbf{B}$$

$$\frac{\partial C}{\partial t} + \mathbf{u}\cdot\nabla C = \frac{E}{Pr}\nabla^2 C + S_{T/\xi}$$

$$\nabla \cdot \mathbf{u} = 0$$

$$\nabla \cdot \mathbf{B} = 0$$

Our first step is to find an initial model that reproduces the present day reversal frequency of ~4 Myr^{-1}. To do so, we set the initial values E=3e-4, Pm=20 and Pr=1. We use no slip and magnetically insulating conditions on both boundaries, set a constant and homogeneous mass anomaly flux through the inner core boundary (ICB) and impose the present-day heat flow distribution at the CMB (Fig. 1, left) (Biggin et al., 2012). We then run a range of numerical models for varying Ra_Q; the model that best reproduces the present-day reversal frequency is our *initial model*.

Next, we compute changes in the dynamo parameters as a function of time, using the combined efforts of Aubert et al. (2009) and Olson et al. (2013). These parameter changes and CMB heat flow distributions of the past 300 Myr from Biggin et al. (2012), enable us to produce dynamo models which potentially reproduce secular changes in the magnetic field. Our final aim is to compute the reversal frequency for the past 300 Myr on the 10 Myr timescale.

CMB heat flow evolution as thermal boundary condition

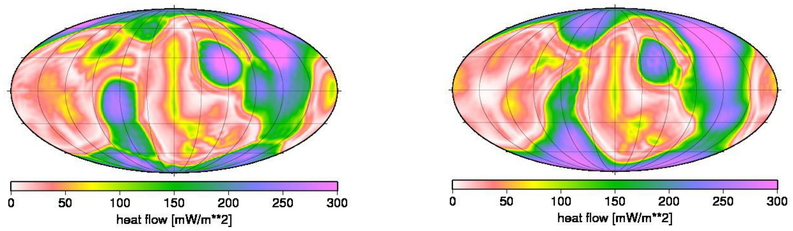

Fig. 1: the present day CMB heat flow distribution (*left*) and at 100 Myr ago (*right*) (Biggin et al., 2012).

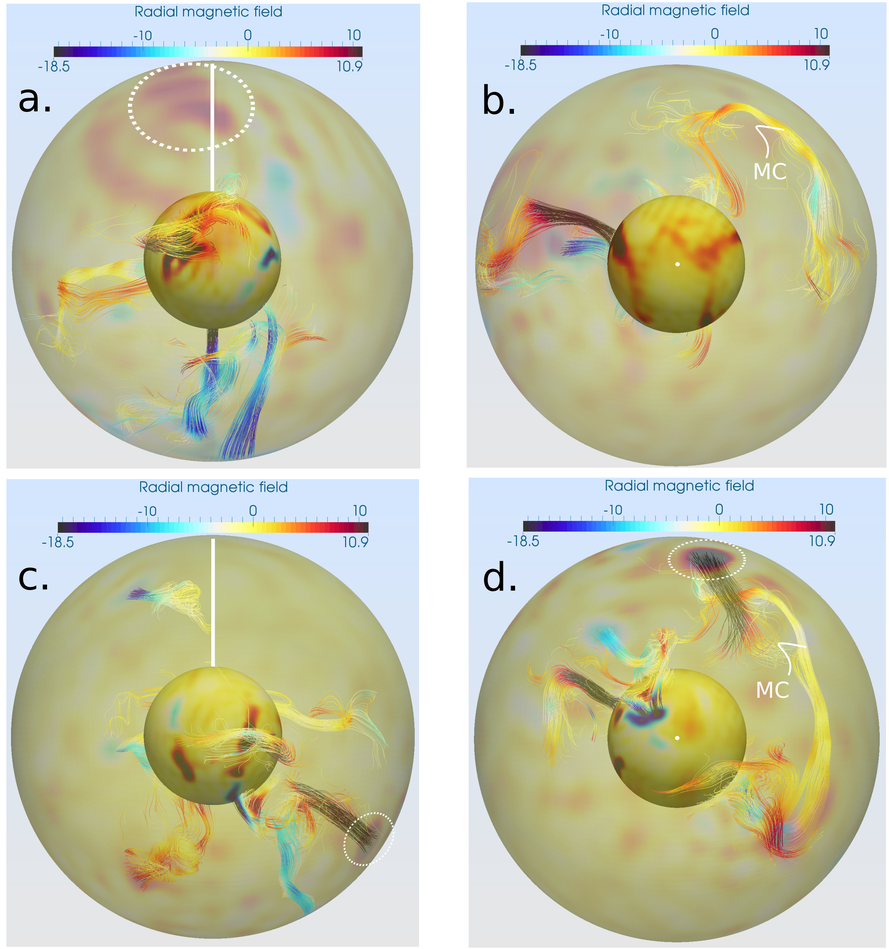

Fig. 2: the radial magnetic field for the initial model during a normal state (a and b) and during a reversal (c and d). The white bar shows the rotation axis. Note that at the CMB the radial magnetic field is characterised by strong anomalies relatively near the equator (c and d, white ellipse), with respect to the normal state (a, white ellipse). In both states, magnetic cyclones (MCs) are noticable in the equatorial plane (Aubert et al., 2008).

Benchmarking results

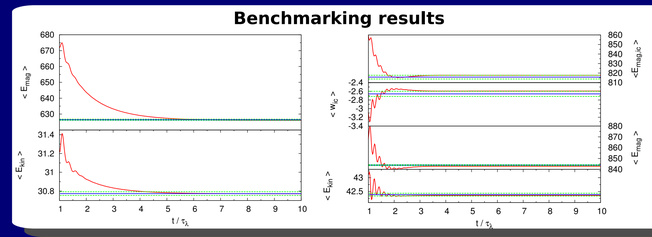

Fig. 3: PARODY-JA benchmark results for the cases 1 (left) and 2 (right) as described in Christensen et al. (2001). The blue and green lines show suggested values and corresponding uncertainty. Quantities converge to the suggested values, implying a succesful benchmark

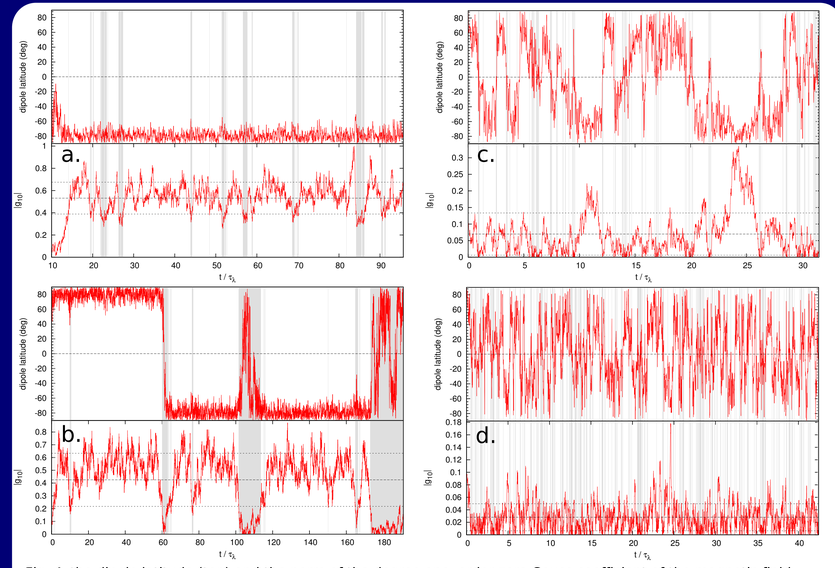

Fig. 4: the dipole latitude (top) and the norm of the degree one, order zero Gauss coefficient of the magnetic field |g10| (bottom) as a function of nondimensional time. Results are shown for Ra_Q=9.9e-5, Ra_Q=1.1e-4, Ra_Q=1.8e-4 and Ra_Q=2.5e-4 (a, b, c and d respectively). Gray areas denote periods at which the dipole field strength is low, in which reversals can occur. Clearly, the reversal frequency increases with the Rayleigh number used, thus with the total CMB heat flow. By matching the computed reversal frequency to the present-day value (~ 4 Myr^{-1}), we aim to find a Rayleigh number corresponding to the present day state of the dynamo.

Results and outlook

Benchmark results show that for both benchmark cases quantities converge to the values suggested by Christensen et al. (2001) (Fig. 3). Therefore, PARODY-JA is correctly installed on our system and produces reliable results.

Moreover, we have found an initial model with Ra_Q=1.2e-4 which corresponds to reversal frequency of 2.1 Myr^{-1}. This is in the required order of magnitude, but we aim to find a better model to fit the present-day frequency. Once a more realistic initial model is found, we will be able to numerical model the magnetic field, in terms of reversal frequency, of the past 300 Myr (see Methods).

Visualisation of the magnetic field in the outer core (Fig. 2) reveals a number of phenomena, such as magnetic up- and downwellings at the ICB and CMB and magnetic cyclones (Aubert et al., 2008). Moreover we find that during a reversal radial magnetic anomalies at the CMB are less likely to be focused at the geographic poles.

Refererences

Aubert, J., Arnou, J., and Wicht, J. (2008). The magnetic structure of convection-driven numerical dynamos. *Geophysical Journal International*, **172**:945-956.

Aubert, J., Labrosse, S., and Poitou, C. (2009). Modelling the paleo-evolution of the geodynamo. *Geophysical Journal International*, **179**:1414-1428.

Biggin, A., Steinberger, B., Aubert, J., Suttie, N., Holme, R., Torsvik, T., Van Der Meer, D., and Van Hinsbergen, D. (2012). Possible links between long-term geomagnetic variations and whole-mantle convection processes. *Nature Geoscience*, **5**(8):526–533.

Olson, P. L., Coe, R. S., Driscoll, P. E., Glatzmaier, G. A., and Robert, P. H. (2010). Geodynamo reversal frequency and heterogeneous core mantle boundary heat flow. *Physics of the Earth and Planetary Interiors*, **180**:66-79.

Olson, P., Deguen, R., Hinnov, L. A., and Zhong, S. (2013). Controls on geomagnetic reversals and core evolution by mantle convection in the Phanerozoic. *Physics of the Earth and Planetary Interiors*, **214**:87-103.

Christensen, U. R., Aubert, J., Cardin, P., Dormy, E., Gibbons, S., Glatzmaier, G. A., Grote, E., Honkura, Y., Jones, C., Kono, M., Matsushima, M., Sakuraba, A., Takahashi, F., Tilgner, A., Wicht, J., and Zhang, K. (2001). A numerical dynamo benchmark. *Physics of the Earth and Planetary Interiors*. **128**:25-34.